

Physics Models in the MARS15 Code for Accelerator and Space Applications*

N.V. Mokhov, K.K. Gudima[†], S.G. Mashnik[‡], I.L. Rakhno, A.J. Sierk[‡], S.I. Striganov

Fermilab, Batavia, IL 60510, USA

[†] *Inst. Appl. Physics, Academy of Sci. Moldova, Kishinev, MD-2028, Moldova*

[‡] *LANL, Los-Alamos, NM 87545, USA*

October 11, 2004

Abstract

The MARS code system, developed over 30 years, is a set of Monte Carlo programs for detailed simulation of hadronic and electromagnetic cascades in an arbitrary geometry of accelerator, detector and spacecraft components with particle energy ranging from a fraction of an electron volt up to 100 TeV. The new MARS15 (2004) version is described with an emphasis on modeling physics processes. This includes an extended list of elementary particles and arbitrary heavy ions, their interaction cross-sections, inclusive and exclusive nuclear event generators, photo-hadron production, correlated ionization energy loss and multiple Coulomb scattering, nuclide production and residual activation, and radiation damage (DPA). In particular, the details of a new model for leading baryon production and implementation of advanced versions of the Cascade-Exciton Model (CEM03), and the Los Alamos version of Quark-Gluon String Model (LAQGSM03) are given. The applications that are motivating these developments, needs for better nuclear data, and future physics improvements are described.

*Presented paper at the *International Conference on Nuclear Data for Science and Technology*, Santa Fe, New Mexico, September 26 - October 1, 2004

Physics Models in the MARS15 Code for Accelerator and Space Applications¹

N.V. Mokhov*, K.K. Gudima[†], S.G. Mashnik**, I.L. Rakhno*, A.J. Sierk** and S.I. Striganov*

*Fermi National Accelerator Laboratory, MS 220, Batavia, Illinois 60510-0500, USA

[†]Institute of Applied Physics, Academy of Sciences of Moldova, Kishinev, MD-2028, Moldova

**Los-Alamos National Laboratory, MS B283, Los-Alamos, New-Mexico 87545, USA

Abstract. The MARS code system, developed over 30 years, is a set of Monte Carlo programs for detailed simulation of hadronic and electromagnetic cascades in an arbitrary geometry of accelerator, detector and spacecraft components with particle energy ranging from a fraction of an electron volt up to 100 TeV. The new MARS15 (2004) version is described with an emphasis on modeling physics processes. This includes an extended list of elementary particles and arbitrary heavy ions, their interaction cross-sections, inclusive and exclusive nuclear event generators, photohadron production, correlated ionization energy loss and multiple Coulomb scattering, nuclide production and residual activation, and radiation damage (DPA). In particular, the details of a new model for leading baryon production and implementation of advanced versions of the Cascade-Exciton Model (CEM03), and the Los Alamos version of Quark-Gluon String Model (LAQGSM03) are given. The applications that are motivating these developments, needs for better nuclear data, and future physics improvements are described.

INTRODUCTION

The MARS code system [1, 2] is designed for detailed simulation of hadronic and electromagnetic cascades in an arbitrary geometry of shielding, accelerator, detector and spacecraft components. The current MARS15 version [3, 4] combines the theoretical models for strong, weak and electromagnetic interactions with matter of hadrons, heavy ions and leptons, and phenomenological models. A system studied can contain up to 10^5 objects, ranging in dimensions from microns to hundreds kilometers and can be made of up to 100 composite materials, with arbitrary 3-D magnetic and electric fields. A powerful Graphical-User Interface is used for visualization of the geometry, materials, fields, particle trajectories, and results of calculations. MARS15 provides five geometry options and flexible histogramming, can use as an input MAD optics files, and provides an MPI-based multiprocessing option and various biasing techniques.

NUCLEAR CROSS-SECTIONS

Total and elastic cross-sections of hadron-nucleon interactions for ordinary hadrons are described using corresponding fits to experimental data. Cross-sections for hyperon-nucleon interactions are described via the ordinary hadron cross-sections using the Additive Quark Model rules. At energies above 5 GeV, such an approach agrees well with data. At lower energies, the hyperon-nucleon cross-sections are very close to proton-nucleon ones. Hadron-nucleus total and inelastic cross-sections at energies above 5 GeV are calculated using the Glauber model. At lower energies, parameterizations to experimental data are used. For neutral kaons, cross-sections on both nucleon and nucleus targets are calculated using the relation based on isospin and hypercharge conjugation. Total and inelastic cross-sections for heavy-ion nuclear interactions are based on the JINR model (see Ref. [4]). Photonuclear interaction cross-sections are described in great details for all nuclei and energies from a few MeV up to 40 TeV using approximations from Ref. [5]. Fig. 1 gives an example of the neutron and heavy-ion cross-section description in the code.

¹ Work supported by the Universities Research Association, Inc., under contract DE-AC02-76CH03000 with the U. S. Department of Energy, and in part by the Moldovan-US bilateral grant program, CRDF projects MP2-3025 and MP3045, and the NASA grant NRA-01-01-ATP-066.

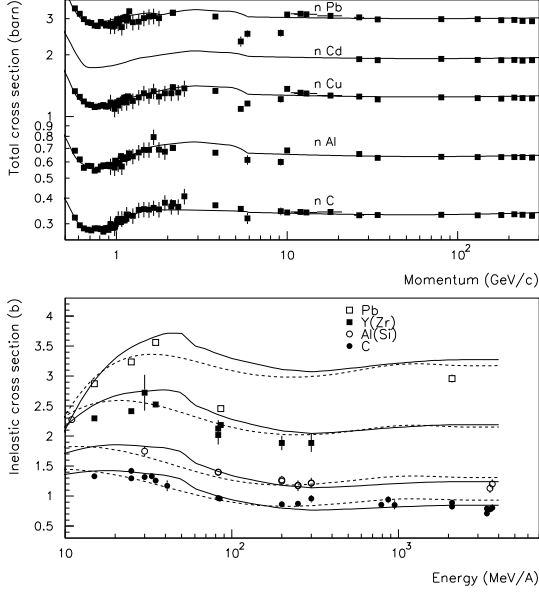


FIGURE 1. Total neutron-nucleus cross-sections (top) and inelastic nuclear cross-sections of ^{12}C ions (bottom) as calculated in MARS15 (solid lines) vs data [6]. Dashed lines are from NASA model (see Ref. [4]).

INCLUSIVE EVENT GENERATOR

Many processes in MARS15, such as electromagnetic showers, most of hadron-nucleus interactions, decays of unstable particles, emission of synchrotron photons, photohadron production and muon pair production, can be treated either analogously or inclusively with corresponding statistical weights. The basic model for the original MARS program [1], introduced in 1974, came from Feynman's ideas concerning an inclusive approach to multiparticle reactions and *weighting* techniques. At each interaction vertex, a particle cascade tree can be constructed using only a fixed number of representative particles (the precise number and type depending on the specifics of the interaction), and each particle carries a statistical weight w , which is equal, in the simplest case, to the partial mean multiplicity of the particular event. Energy and momentum are conserved *on average* over a number of collisions. It was proved rigorously that such an estimate of the first moment of the distribution function is unbiased [7].

Inclusive particle production in nuclear interactions above 3 GeV is modeled in MARS15 using the following form for double differential distributions:

$$\frac{d^2 N^{pA \rightarrow pX}}{dp d\Omega} = R^{pA \rightarrow pX}(A, E_0, p, p_\perp) \frac{d^2 N^{pp \rightarrow pX}}{dp d\Omega}.$$

Differential cross-sections on a hydrogen target are described by a set of models and phenomenological for-

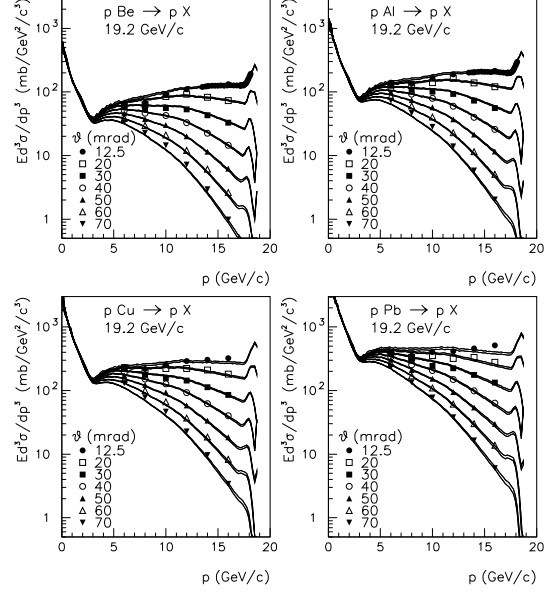


FIGURE 2. Invariant cross-sections for $pA \rightarrow pX$ reactions at 19.2 GeV/c in MARS15 (lines) vs data [8].

mulae. For example, proton production in pp -collisions $\frac{d^2 N^{pp \rightarrow pX}}{dp d\Omega}$, is described with a high accuracy in four kinematic regions of Feynman's $x_F = |p_L^*/p_{max}^*|$:

1. Resonance region $x_F > 1 - 2.2/p_0$, a sum of five baryon resonances, Breit-Wigner formulae.
2. Diffractive dissociation region $1 - 2.2/p_0 < x_F < 0.9$, triple-Reggeon formalism.
3. Fragmentation region $0.4 < x_F < 0.9$, phenomenological model with flat behavior on longitudinal and exponential on transverse momenta.
4. Central region $0 < x_F < 0.4$, fit to experimental data with normalizations at $x_F = 0$ and $x_F = 0.4$.

A nuclear modification factor $R^{pA \rightarrow pX}$ is known much better than the absolute yields, and its dependence on particle momenta p_\perp , p_0 , and p is much weaker than for the differential cross-sections themselves. For example, for $pA \rightarrow pX$, it is presented in a factorized form

$$R^{pA \rightarrow pX} = F(p/p_0) \left(\frac{A}{2}\right) \alpha p_T^2 \left(\frac{A}{9}\right) \gamma(E_0).$$

A momentum dependence is given by the Additive Quark Model. Quasi-elastic scattering is modeled additionally. A quality of this model is demonstrated in Fig. 2.

EXCLUSIVE EVENT GENERATOR

The 2003 version of the improved Cascade-Exciton Model [9] code, CEM03, combined with the Fermi break-

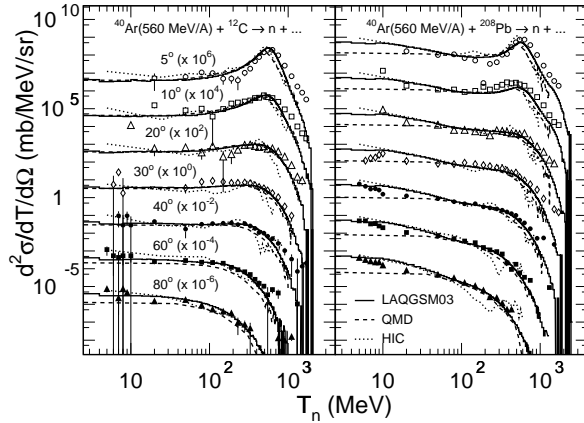


FIGURE 3. Differential cross-sections of neutrons in 560 MeV/A $Ar + C$ and $Ar + Pb$ reactions as calculated with LAQGSM03, QMD [12] and HIC [13] codes vs data [14].

up model, the coalescence model, and an improved version of the Generalized Evaporation-fission Model (GEM2) is used as a default for hadron-nucleus interactions below 5 GeV. The 2003 version of the Los Alamos Quark-Gluon String Model [10] code, LAQGSM03, was implemented into MARS15 for particle and heavy-ion projectiles at 10 MeV/A to 800 GeV/A. This provides a power of full theoretically consistent modeling of exclusive and inclusive distributions of secondary particles, spallation, fission, and fragmentation products (see Refs. [3, 4]). The following modules have been improved recently in this package: intra-nuclear cascade (angular distributions); complex particle emission algorithms; photonuclear modeling at 30 MeV to 2 GeV in CEM; and a hydrogen target mode. Figs. 3 and 4 show benchmarking results for neutron and nuclide production in heavy-ion nuclear interactions. Further developments of this package are underway.

For several years MARS is linked to the Dual-Parton Model code [11], DPMJET3, for the very first vertex in a cascade tree. This is used in our numerous studies for the LHC 7×7 TeV collider and its detectors, and at very high energies up to 100 TeV.

ELASTIC SCATTERING

The elastic model at $E < 5$ GeV is based on evaluated nuclear data from the LA-150 and ENDF/HE-VI libraries [16] and from other sources (see Ref. [17]). For protons, the interference of nuclear and Coulomb elastic scattering is taken into account. An example is shown in Fig. 5. At $E > 5$ GeV, a simple analytical description used in the code for the coherent component of scattering cross-sections is quite consistent with data.

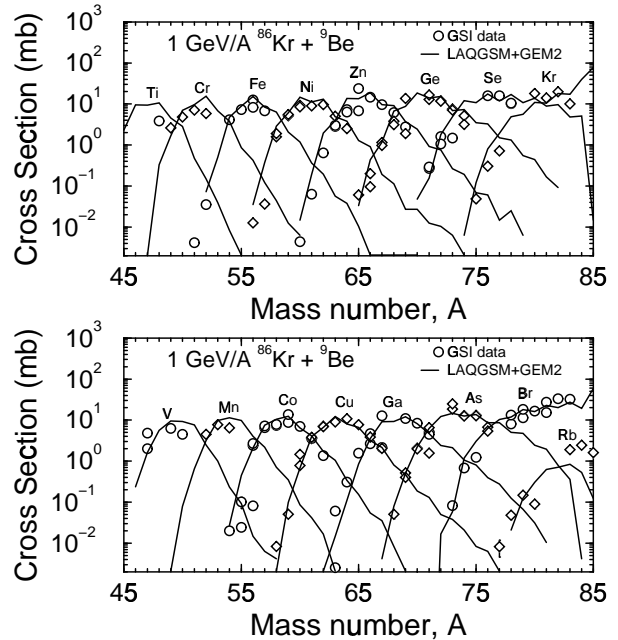


FIGURE 4. Mass yield in $^{86}Kr + ^9Be$ reaction at 1 GeV/A as calculated with LAQGSM03 and measured in Ref. [15].

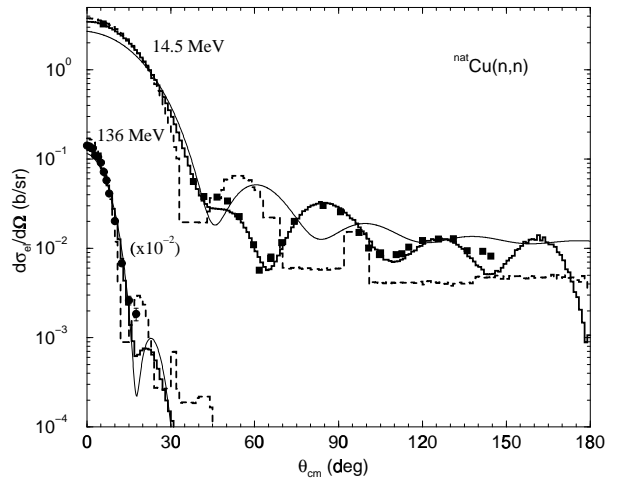


FIGURE 5. Neutron elastic scattering distributions on copper calculated with MARS15 (thick solid line), LAHET (dashed line) and Sychev formula (thin line) vs data (symbols) (see Ref. [17]).

LOW-ENERGY NEUTRONS

Once the energy of neutrons falls below 14 MeV, all subsequent neutron interactions are described using the appropriate MCNP4C [18] modules. Secondaries generated at this stage by neutrons – protons, photons and deuterons – are directed back to the MARS modules for a corresponding treatment. This implementation, along

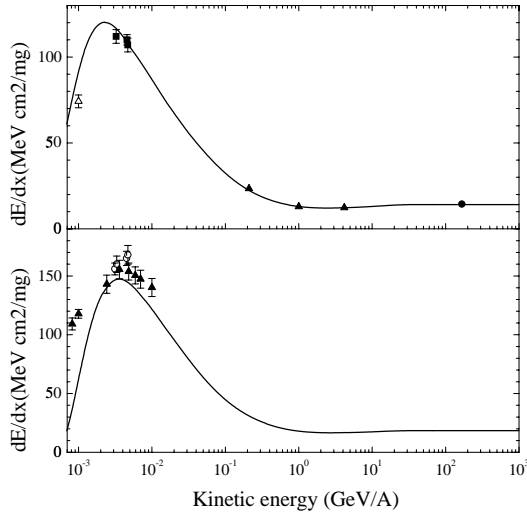


FIGURE 6. Mean ionization energy loss for lead ions in aluminum (top) and for ^{238}U ions in carbon (bottom) as calculated in MARS15 and measured (see Ref. [4]).

with algorithms developed for heavier recoils and photons from the thermal neutron capture on ^6Li and ^{10}B , allows the detailed description of corresponding effects in hydrogenous, borated and lithium-loaded materials. The interface includes several other modifications to the dynamically allocated storage, material handling, as well as an optional writing of low-energy neutrons and other particles to a file for further treatment by a stand-alone MCNP code if needed.

ELECTROMAGNETIC PROCESSES

The mean ionization energy loss for charged particles, except for heavy ions, is calculated using Bethe formalism with the density correction. For heavy ions – as described in Ref. [4] – the Lindhard-Sorensen correction to the regular ionization logarithm and Barkas term are taken into account. In addition, at low ion kinetic energies, the processes of electron capture and loss are accounted for by means of an effective ion charge. The effective charge, z_{eff} , is determined according to semi-empirical formulae and used instead of a bare ion charge. The projectile nuclear form-factor is also taken into account. Comparison between calculated stopping power and data for lead and uranium ions is given in Fig. 6.

A new algorithm [19] for modeling correlated ionization energy loss and multiple Coulomb scattering was implemented in MARS15 for arbitrary mixtures. It takes into account arbitrary projectile and nuclear target charge distributions, exact kinematics of projectile-electron interactions, nuclear screening, projectile-electron interac-

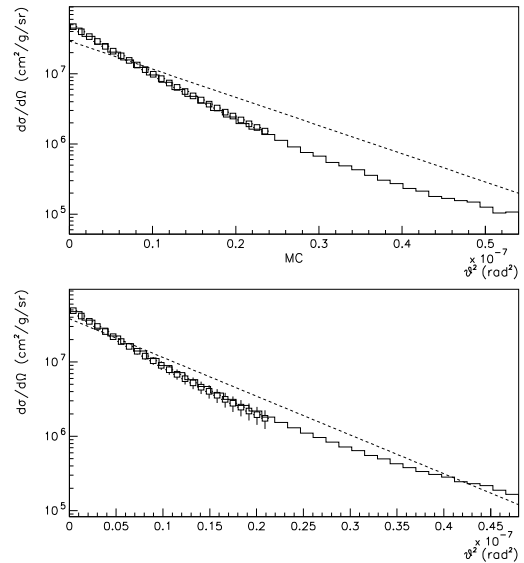


FIGURE 7. Coulomb scattering of 70-GeV protons on $0.1X_0$ thick hydrogen (top) and lead (bottom) targets as calculated in MARS15 (solid histogram) and with a standard Gaussian (dashed line) and measured in Ref. [20].

tions, and accurately treats both soft and hard collisions. Calculated correlations between energy loss and scattering are quite substantial for low-Z targets. A comparison of new results with data is shown in Fig. 7 along with the Rossi distribution.

Radiative processes for single-charged particles and heavy ions – bremsstrahlung and direct pair production – are modeled directly [7].

RESIDUAL DOSE

A substantially improved ω -factor based algorithm [21] to calculate residual dose rates in arbitrary composite materials for arbitrary irradiation and cooling times was developed and implemented into MARS15. The algorithm distinguishes three major energy groups responsible for radionuclide production: (1) above 20 MeV, (2) 1 to 20 MeV, and (3) below 0.5 eV. Creation of the residual nuclides was pre-calculated with the FLUKA code for cascades induced by energetic hadrons in cylindrical samples of 17 elements: C, O, Na, Mg, Al, Si, K, Ca, Cr, Fe, Ni, Cu, Nb, Ag, Ba, W, Pb. The emission rates of de-excitation photons were determined for irradiation time $12 \text{ hours} < T_i < 20 \text{ years}$ and cooling time $1 \text{ sec} < T_c < 20 \text{ years}$. Corresponding dose rates on the outer surfaces are calculated from photon fluxes and related to the star density above 20 MeV (first group), and neutron fluxes in two other energy groups.

RADIATION EFFECTS

Radiation damage to material – displacements per atom (DPA) – is calculated in MARS15 within a damage energy concept, taking into account recoil nuclei in elastic and inelastic hadron-nucleus interactions. Although this is a rather adequate approach for many applications, further developments to the model, *e.g.*, a gamma-induced radiation damage channel, are underway.

A model to simulate single event upsets (SEU) in electronic devices is under development. It employs a sharp threshold function for an upset probability and complete 3-D modeling of heavy-ion transport and ionization loss in microscopic electronic structures. Currently in MARS15, the energy threshold for heavy ions is as low as 100 keV per nucleon and, therefore, the SEU model is adequate when ions of medium and high energies dominate, *i.e.* for space applications.

THICK TARGET BENCHMARKING

New photonuclear algorithms in MARS15 for interaction cross-sections and hadron production have been recently tested by the KEK colleagues (T. Sanami). Neutron spectra at three angles have been calculated with the MARS15 and MCNPX codes for a 2-GeV electron beam on a 10 radiation length thick copper target. Fig. 8 shows calculated results in comparison with experimental data [22]. Results are in a good agreement at all neutron energies except for the middle of the energy region at smallest angle where calculations slightly underestimate the data. Further analysis is needed.

Second thick target test concerns benchmarking the heavy-ion interaction and transport algorithms in MARS15. Fig. 9 shows neutron yield from a lead cylinder of 20-cm diameter and 60-cm thick irradiated by 0.5 to 3.65 GeV/A light ion beams. Our results are in a good agreement with data [23] and predictions of the latest version of the SHIELD code [24] presented in Ref. [25].

APPLICATIONS

Major MARS15 applications include: operational and accidental/destructive beam loss, collimation, targetry (yield and material integrity), radiation damage in materials (DPA) and electronics (SEU), shielding (including deep penetration), activation, environment (ground water etc), protection of superconducting magnets (quench stability and dynamic heat loads), proton radiography, neutrino-induced radiation hazard, background minimization in collider and fixed-target experiments, neu-

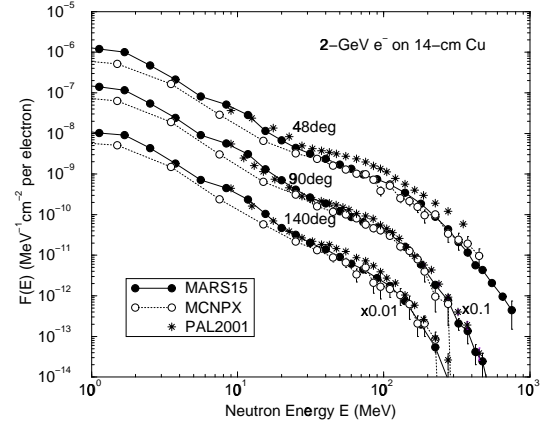


FIGURE 8. Neutron spectra calculated with MARS15 and MCNPX at three angles for a 2-GeV electrons on a thick copper target vs data [22].

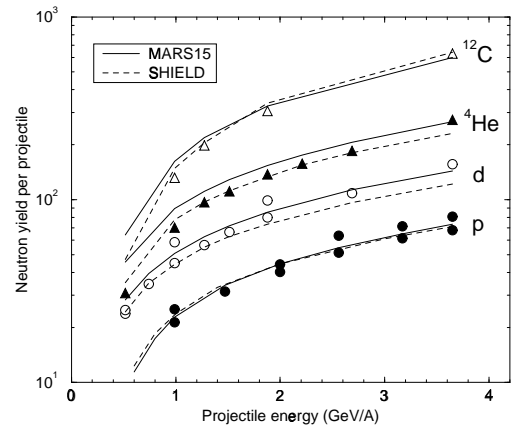


FIGURE 9. Calculated with MARS15 and SHIELD and measured in Ref. [23] total neutron yield ($E < 14.5$ MeV) from a lead cylinder vs ion beam energy.

trino experiments, cosmic rays and space exploration. Specific recent applications were as follows:

Accelerators. Fermilab ($E_0 = 5$ MeV to 1000 GeV), Proton Driver (up to 8 GeV), LHC at CERN (up to 7 TeV per beam), J-PARC and KEK in Japan ($E_0 = 0.4$ to 50 GeV), Spallation Neutron Source at ORNL, Rare Isotope Accelerator at ANL/MSU (up to 1 GeV/A), Advanced Photon Source at ANL ($E_e \leq 8$ GeV), Los Alamos, e^+e^- Linear Colliders, $\mu^+\mu^-$ collider and neutrino factories.

Experiments and Detectors. Collider experiments CDF, DØ, BTeV, CMS, ATLAS; neutrino experiments NuMI/MINOS, MiniBooNe and J-PARC, etc.

Space. Supernova Acceleration Project (SNAP) and cosmic rays in atmosphere

PLANS AND NEEDS FOR DATA

The following nuclear physics model developments in the MARS15-CEM03-LAQGSM03 package are underway: multi-fragmentation, photonuclear interactions below 30 MeV and above 2 GeV, diffraction, Coulomb-induced fission and electromagnetic dissociation for heavy projectiles. Better nuclear data are needed on nuclide production cross-sections at 200-500 MeV/A, complex particle and fragment spectra above 2.5 GeV, hadron differential cross-sections in hadron-nucleus interactions at zero angles, and at large angles ($x_F < 0$), neutral kaon production, and heavy-ion total and elastic cross-sections. Other needs for data include effective ion charge and, even better, ion charge distributions in various target materials including gases for heavy ions below a few MeV/A, angle-energy loss correlations, and DPA and SEU in important materials and components at medium and high energies.

REFERENCES

1. Mokhov, N. V., "Monte-Carlo Modeling of Particle Distributions in Accelerator Shielding at 50 MeV to 1500 GeV," in *IV All-Union Conf. on Charged Particle Accelerators*, Nauka, Moscow, 1975, pp. 222–226.
2. Mokhov, N. V., The MARS Code System User's Guide, Tech. rep., Fermilab-FN-628 (1995), URL <http://www-ap.fnal.gov/MARS/>.
3. Mokhov, N. V., Gudima, K. K., James, C. C., Kostin, M. A., Mashnik, S. G., Ng, E., Ostiguy, J.-F., Rakhno, I. L., Sierk, A. J., and Striganov, S. I., Recent Enhancements to the MARS15 Code, Tech. rep., Fermilab-Conf-04/053 (2004).
4. Mokhov, N. V., Gudima, K. K., Mashnik, S. G., Rakhno, I. L., and Striganov, S. I., Towards a Heavy-Ion Transport Capability in the MARS15 Code, Tech. rep., Fermilab-Conf-04/052 (2004).
5. Kossov, M. V., *Eur. Phys. J.*, **A14**, 377–392 (2002).
6. Barashenkov, V. S., *Cross-Sections of Particle and Nuclei Interactions with Nuclei*, Joint Institute for Nuclear Research, Dubna, Russia, 1993.
7. Kalinovskii, A. N., Mokhov, N. V., and Nikitin, Y. P., *Passage of High-Energy Particles through Matter*, AIP, New York, 1989.
8. Allaby, J. V., Binon, F., Diddens, A. N., Duteil, P., Kloving, A., Meunier, R., Peigneux, J. P., Sacharidis, E. J., Schlüpmann, K., Spighel, M., Stroot, J. P., Thorndike, A. M., and Wetherell, A. M., High-Energy Particle Spectra from Proton Interactions at 19.2 GeV/c, Tech. rep., CERN-70-12 (1970).
9. Mashnik, S. G., and Sierk, A. J., "CEM2k - Recent Developments in CEM," in *Accelerator Applications*, E-print: nucl/th/0011064, Washington, DC, 2000, pp. 328–341.
10. Gudima, K. K., Mashnik, S. G., and Sierk, A. J., User Manual for the Code LAQGSM, Tech. rep., LA-UR-01-6804 (2001).
11. Roesler, S., Engel, R., and Ranft, J., "The Event Generator DPMJET-III at Cosmic Ray Energies," in *ICRC-2011 Conference*, Copernicus Gesellschaft, 2001, p. 439.
12. Niita, K., Chiba, S., Maruyama, T., Takada, H., Fukahori, T., Nakahara, Y., and Iwamoto, A., *Phys. Rev.*, **C52**, 2620 (1995).
13. Bertini, H. W., Gabriel, T. A., Santoro, R. T., Hermann, O. W., Larson, N. M., and Hunt, J. M., HIC-1: A First Approach to the Calculation of Heavy-Ion Reactions at Energies ≥ 50 MeV/Nucleon, Tech. rep., ORNL-TM-4134 (1974).
14. Iwata, Y., Murakami, T., Sato, H., Iwase, H., Nakamura, T., Kurosawa, T., Heibronn, L., Ronningen, R. M., Ieki, K., Tozawa, Y., and Niita, K., *Phys. Rev.*, **C64**, 054609 (2001).
15. Voss, B., *Untersuchung der Projektilfragmentation und der Isotopenrennung relativistischer Schwerionen am Fragmentseparator der GSI*, Ph.D. thesis, Institute für Kernphysik Technische Hochschule Darmstadt, Darmstadt (1995), URL <http://www-wnt.gsi.de/kschmidt/theses.htm>.
16. Chadwick, M. B., Young, P. G., Chiba, S., Frankle, S. C., Hale, G. M., Hughes, H. G., Koning, A. J., Little, R. C., MacFarlane, R. E., Prael, R. E., and Waters, L. S., *Nucl. Sci. Eng.*, **131**, 293 (1999).
17. Rakhno, I. L., Mokhov, N. V., Sukhovitski, E., and Chiba, S., "Simulation of Nucleon Elastic Scattering in the MARS14 Code System," in *ANS Topical Meeting on Accelerator Applications/Accelerator Driven Transmutation Technology Applications*, *AccApp/ADTTA'01*, ISBN: 0-89448-666-7, Omnipress CD ROM (2002), Reno, Nevada, 2001.
18. Briesmeister, J. F., MCNP - A General Monte Carlo N-Particle Transport Code, Version 4C, Tech. rep., Pub. LA-13709-M (2000).
19. Striganov, S. I., On the Theory and Simulation of Multiple Coulomb Scattering of Heavy Particles, Tech. rep., Fermilab-Conf-04/056 (2004).
20. Shen, G., Ankenbrandt, C., Atac, M., Brown, R., Ecklund, S., Gollon, P., Lach, J., MacLachlan, J., Roberts, A., Fajardo, L., Majka, R., Marx, J., Nemethy, P., Rosselet, L., Sandweiss, J., Schiz, A., and Slaughter, A., *Phys. Rev.*, **D85**, 1584–1588 (1979).
21. Rakhno, I., Mokhov, N., Elwyn, A., Grossman, N., Huhtinen, M., and Nicolas, L., "Benchmarking Residual Dose Rates in a NuMI-like Environment," in [17].
22. Lee, H.-S., Ban, S., Sanami, T., Takahashi, K., Sato, T., K.Shin, and Chung, C., *J. Nucl. Sci. Tech.*, **Suppl. 4**, 10–13 (2004).
23. Vassil'kov, R. G., and Yurevich, V. I., "Neutron Emission from an Extended Lead Target under the Action of Light Ions in GeV Region," in *ICANS-XI*, KEK, Tsukuba, Japan, 1990, p. 340.
24. Dementyev, A. V., and Sobolevsky, N. M., *Radiation Measurements*, **30**, 553–557 (1999).
25. Sobolevsky, N. M., and Mustafin, E., "Monte Carlo Calculation of Neutron Yield from Extended Iron and Lead Targets Irradiated by 1 and 3.65 GeV/u Ion Beams," in *International Workshop on Nuclear Data for the Transmutation of Nuclear Waste*, ISBN 3-00-012276-1, GSI, Darmstad, Germany, 2003, URL <http://ww-wnt.gsi.de/tramu/>.